4.4.3. Optimum Optical Thickness

(1) Dynamic range

The cloud top height can be roughly modeled between 0.2 atm and 1 atm assuming clouds exist only in the troposphere. The possible observation geometries from a satellite for low-Earth orbits are listed in Table 4-6.

Table 4-6. Possible observation geometries to be considered for cloud detection.

Cloud height (atm)	0.2- 1
Solar Zenith angle (deg)	0- 80
Viewing angle (deg)	0 – 60
Air mass factor without considering scattering	0.4 - 6

(2) Sensitivity

An optical thickness that has maximum sensitivity has to be carefully selected since the dynamic range available on board is limited because of the difficulty in tuning the electronics. The possible range of transmittance can be described as follows if the air mass factor is between 0.4 and 6 as indicated in Table 4-6.

$$\Delta T = exp(-0.4X) - exp(-6X). \tag{4-7}$$

The optical thickness for an air mass factor of 1 should be (X=) 0.48 to maximize the dynamic range as indicated in the following equation.

$$dT / dX = -0.4\,exp(-0.4X) + 6\,exp(-6X) = 0. \tag{4-8}$$

The proposed cloud detection system has suitable sensitivity if the convoluted optical thickness using a filter radiometer is about 0.5 as described in section 3.6.

4.4.4. Fraction Retrieval of Thick Clouds

Thick cloud fraction retrieval is discussed in Chapter 3. Figure 4-19 illustrates the fitting process of cloud fraction and height. The deviation of the calculated value from the observed value is normalized by the observed value in the fitting process, as demonstrated below.

$$\chi^2 = \sum_{j=1}^{M} \left(\frac{R_{obs}(j, h_i, \alpha_{ij} r_i) - R_{calc}(j, h_i, \alpha_{ij} r)}{R_{obs}(j, h_i, \alpha_{ij} r_i)} \right)^2 / M \tag{4-9}$$

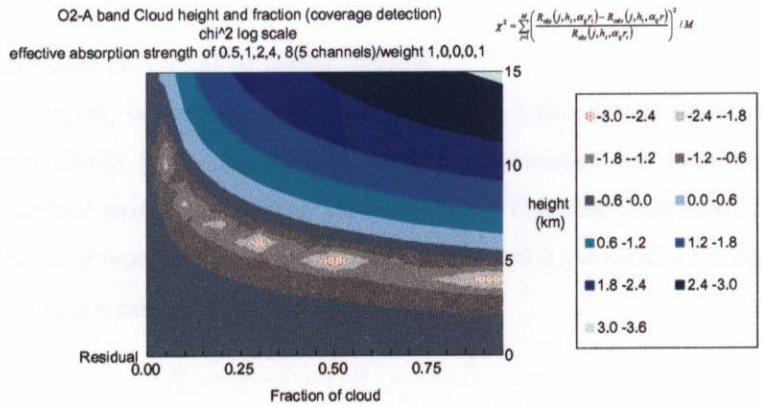

Figure 4-19. The sum of the earth's albedo deviation at O_2 *A* band channels, which is minimized in the fitting process to determine the cloud coverage and cloud height.

4.4.5. Cloud-Top and Aerosol Height Retrieval

(1) Spectral characteristics of clouds and aerosol

Figure 4-20 depicts the spectral characteristics of the MODTRAN aerosol model. The model demonstrates that there is no unique spectral characteristic structure in the visible and UV regions. Therefore, the retrieved characteristics in O_2 *A* can be extended in the UV region and are useful for cloud and aerosol correction.

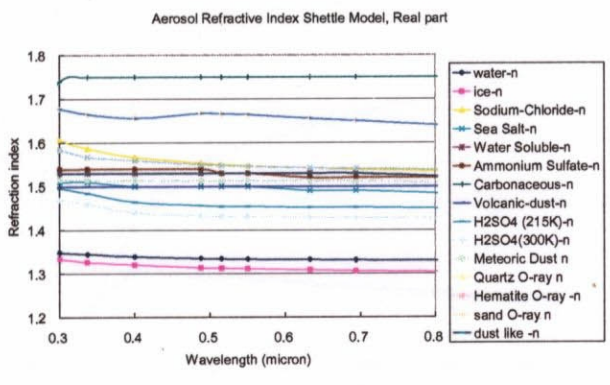

(a)

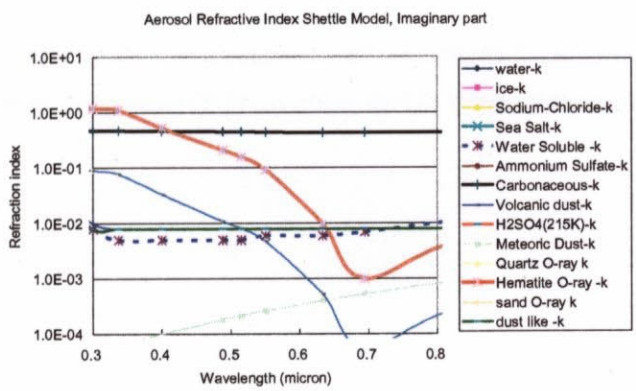

(b)

Figure 4-20. Refraction index of MODTRAN aerosol model: (a) real part and (b) imaginary part.

(2) Stratospheric aerosol retrieval in polar region

Regarding polar region, where surface albedo might has seasonal variation and is not modeled as Lambertian, the surface albedo (R_s in equation (4-1)) is the parameter that must be retrieved with each measurement. When aerosol exists, the surface albedo retrieval becomes complicated. If an aerosol layer exists at high altitude, in other words, above the scattering height and it has no absorption, the earth's albedo of ozone (O_3) insensitive channels can be expressed as follows.

$$R_e = (1-t) + t^2 R_{ef} \frac{1}{1-(1-t)R_{ef}}, \qquad (4\text{-}10)$$

where t is the transmittance of the aerosol layer and R_{ef} is the earth's albedo of aerosol free.

Figure 4-21 shows the spectral characteristics of each item in equation (5-1) except for R_s and t. The spectral dependency will be applied to discriminate between the aerosol transmittance and the surface albedo. Figure 4-22 shows the earth's albedo deviation, which is minimized in the fitting process to determine the surface albedo of 0.2 and the aerosol transmittance of 0.5, assuming that the surface albedo and aerosol transmittance do not have spectral dependency. The proper combination is deeper in the contour plot of Figure 4-22 and the solution is unique. After launch, the operational software will search the minimum deviation and estimate the surface albedo and the aerosol transmittance at the same time. The spectral channels in the whole spectral region except for O_3 sensitive channels will be used in this fitting process.

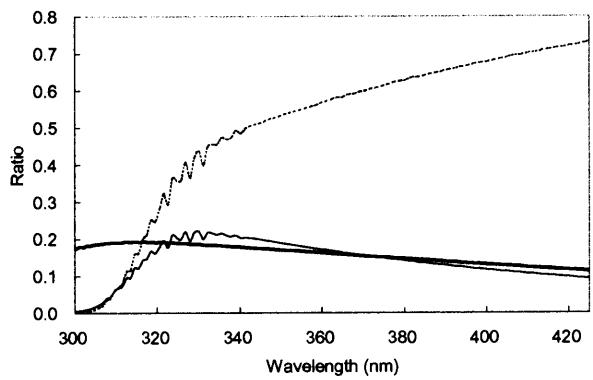

Figure 4-21. Simulated spectral characteristics of normalized I_a (solid line), FT_a (dotted line), and T_b (bold line) in equation (5-1) assuming the US standard atmosphere.

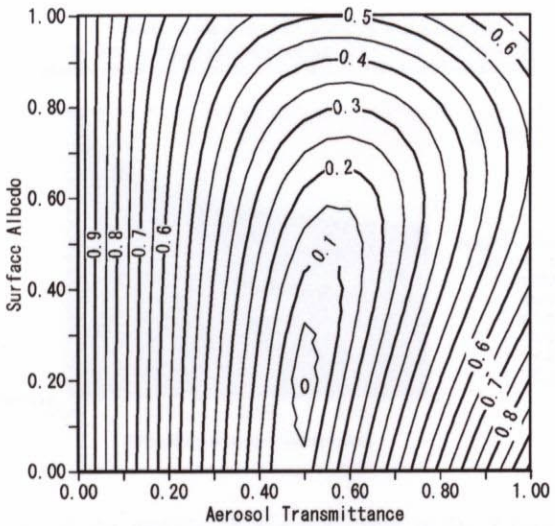

Figure 4-22. The sum of the earth's albedo deviation, which is minimized in the fitting process to determine the surface albedo of 0.2 and the aerosol transmittance of 0.5.

(3) Thin cloud and tropospheric aerosol retrieval

Thin cloud and tropospheric aerosol retrieval is discussed next. Figure 4-23 shows the χ^2 variation of the fitting process for thin cloud and aerosol height and albedo (reflectivity) retrieval. The results indicate that a large variation of optical thickness in the convoluted O_2 *A* band spectra improves the accuracy of height detection. The CloudSat Profiling A-Band Spectrometer/Imager (PABSI) proposed uses this approach [*Heidinger and Stephens*, 2000]. However, a spectral resolution of 0.1 cm^{-1} by a large spectrometer is necessary to achieve an optical thickness of 10. Our approach uses a moderate spectral resolution filter radiometer, which has a very high SNR.

The surface albedo is closely related to the scene averaged optical thickness. Our application is O_3 column density measurements, and thus *a priori* information on the reflectance of the cloud surface and aerosol is important for effective optical path correction.

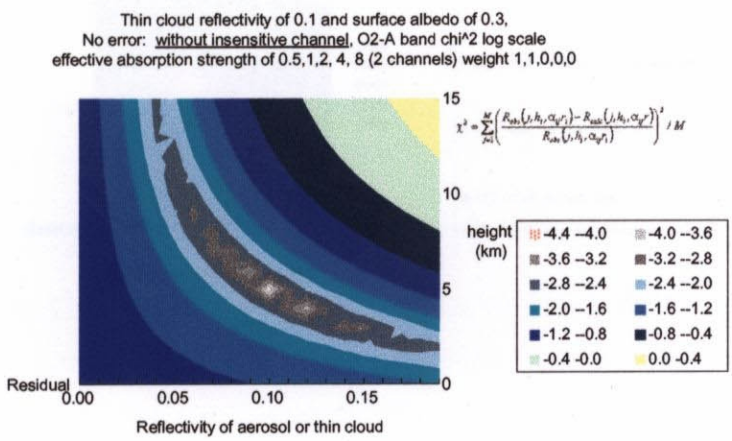

(a)

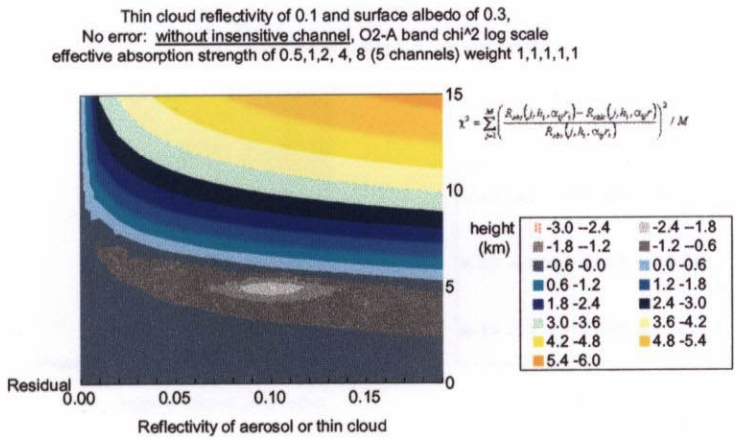

(b)

Figure 4-23. The sum of the earth's albedo deviation at O_2 *A* band channels, which is minimized in the fitting process to determine the reflectivity of thin cloud or aerosol and cloud height: (a) with 2 channels and (b) with 5 channels.

4.4.6. Two-layer Cloud-Heights Retrieval

Most of Earth's surface is covered with thin clouds, such as cirrus, and a thick lower cloud often exists under the thin cloud. This type of cloud cannot be detected when using one spectral pair. Two-layer cloud heights could be retrieved here by using at least two spectral pairs and assuming that the thin cloud thickness and phase function could be properly modeled. Figure 4-24 depicts the simulated results of the χ^2 variation for two-layer cloud heights. The forward calculation assumes the surface albedo value of both the upper thin and lower thick clouds. The amount of O_3 existing between the clouds can be retrieved from the heights of the upper and lower clouds.

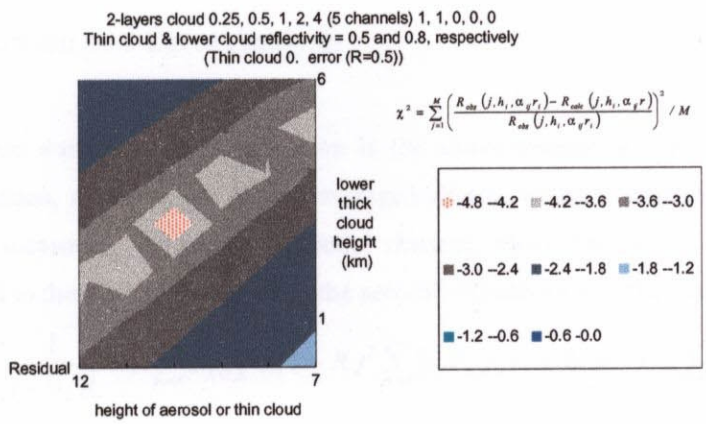

(a)

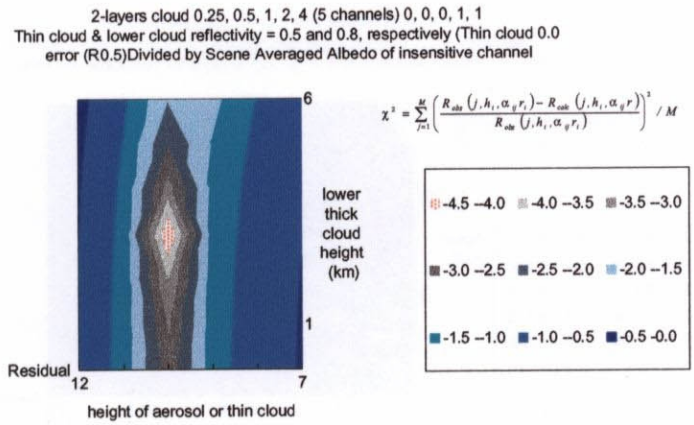

(b)

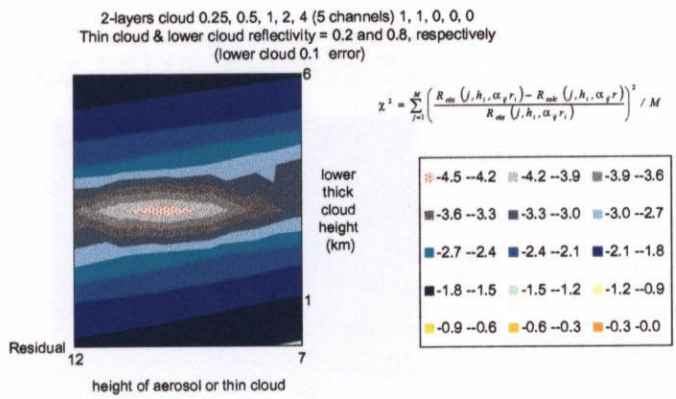

(c)

Figure 4-24. The sum of the earth's albedo deviation at O_2 *A* band channels, which is minimized in the fitting process to determine the cirrus (upper) cloud and lower layer cloud heights: (a) upper cloud reflectivity of 0.5 using 2 optically thin spectral pairs and (b) 2 optically thick spectral pairs, and (c) the upper cloud reflectivity of 0.2.

4.4.7. Scene-Averaged Albedo and Error Analysis

(1) Error estimation

The surface albedo value was assumed to be known in the above simulation. However, the actual surface albedo, such as vegetation, may change. Scene-averaged albedo, which is described below, can be measured simultaneously by measuring the adjacent spectral channel, which has no O_2 absorption. The scene-averaged albedo is equal to the surface albedo when the aerosol reflectivity is sufficiently small.

$$I_{\Omega,h} = (1-R)^2 \sum \beta_\lambda F_\lambda f_\lambda \frac{1}{1-\beta_\lambda R} + R \sum F_\lambda f_\lambda \cong (1-R)^2 \sum \beta_\lambda F_\lambda f_\lambda (1+\beta_\lambda R) + R \sum F_\lambda f_\lambda . \quad (4\text{-}11)$$

The surface albedo cannot be retrieved explicitly in presence of aerosol, as indicated in the above equation. Figure 4-25 illustrates the χ^2 variation with a surface albedo model error of 5%. The combined measurements of various optical thickness pairs that are divided by scene averaged albedo are necessary to improve the aerosol and cloud-height accuracy.

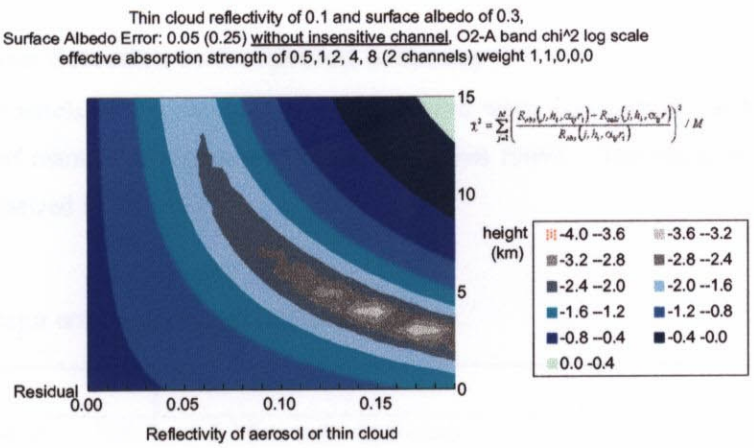

(a)

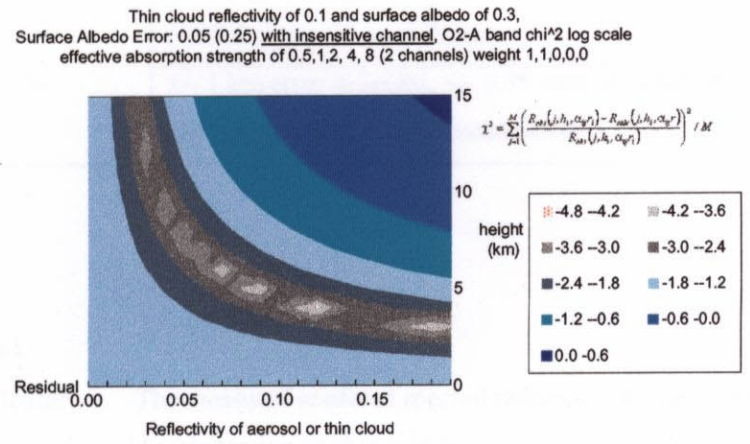

(b)

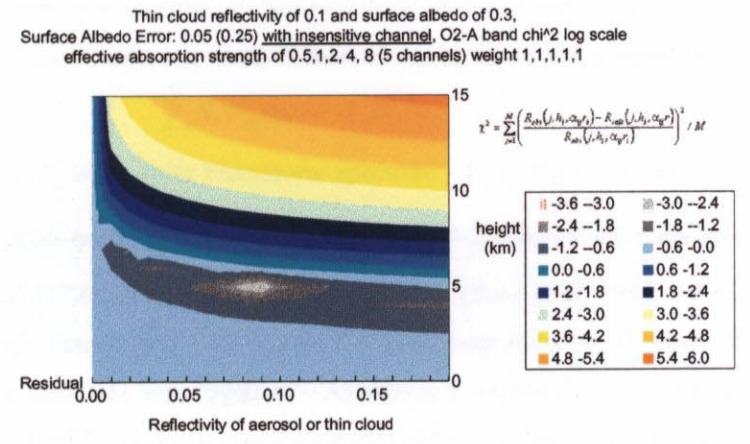

(c)

Figure 4-25. The sum of the earth's albedo deviation at O_2 *A* band channels, which is minimized in the fitting process to determine the reflectivity of thin cloud or aerosol and cloud height. The surface albedo is an unknown parameter and the error of model albedo is 5 % in this case: (a) using 2 channels of the optical thickness of 0.5 and 1.0, (b) using 2 channels of optical thickness of 0.5 and 1.0 divided by the scene averaged albedo, and (c) using 5 channels of optical thickness of 0.5, 1, 2, 4, and 8 divided by the scene averaged albedo.

(2) Improvement of cloud detection and expected accuracy

No more than three channels can be obtained in the O_2 *A* band when very narrow band-pass filters are used, due to the limitation of manufacturing narrow optical band-pass filters. The major error sources and expected accuracy are summarized in Table 4-7.

Table 4-7. The major error sources and expected accuracy.

Error source	Error effect
Vertical temperature profile +/- 10K	+/- 0.15 m error in altitude
Deviation from surface albedo database: +/- 5% Other systematic errors: 1%	+/- 2 km error in height, +/-0.1 error in cloud reflectivity (with 2 channels, no differential)
	+/- 1 km error in height, +/- 0.05 error in cloud reflectivity (with 3 channels, 2 differential pairs)

4.5. O_3 Retrieval

4.5.1. Total O_3 Retrieval

Radiative transfer calculation. The measured scattered spectral radiance is the convolution of the solar Fraunhofer spectra, the slit function, and O_3 absorption as shown below.

(Solar Fraunhofer spectra) $\otimes$ *(Slit Function)* $\otimes$ *(O_3 absorption)*

Upwelling and downwelling fluxes within one spectral channel can be expressed in equation (4-12).

$$\sum S_\lambda F_\lambda \exp(-X_\lambda \alpha_\lambda), \tag{4-12}$$

where S_λ is the slit function, F_λ is the solar Fraunhofer spectrum, X_λ is the O_3 amount on the optical path, and α_λ is the O_3 absorption cross-section. Figure 4-26 and Figure 4-27 show the O_3 absorption cross-section and Fraunhofer spectra around 317.6 nm and 322.4 nm, respectively [*Bass et al*, 1985 and K. Chance, private communication, 2002]. In addition, Figure 4-28 plotted the instrument function, O_3 absorption cross section and solar Fraunhofer spectra near 322 nm, together. As shown in Figure 4-27, Fraunhofer spectra have a random structure [*Berk et al.*, 1989]. In order to calculate the radiance of each spectral channel accurately, the spectral radiance has to be calculated with fine spectral steps less than 0.01 nm that can reproduce the Fraunhofer line spectra and instrument function. However, in ADEOS/TOMS data processing, due to calculation time limitation, the spectral radiance was calculated in the 0.4 nm step with weight assuming the Fraunhofer line is random like structure and instrument function has Gaussian like shape. Instead of calculating with 0.01 nm steps, the effective center wavelength can be defined for the radiative transfer calculation to save computation time. The effective center wavelength is defined as the wavelength which gives the same earth's albedo as the convoluted one with a fine step in the case of total O_3 275 DU and the air mass factor of 2.8. The error due to the simplification is less than 0.1 % over a 100-500 DU range and air mass factor 2-8. For example, the effective

center wavelength of the 322.5 nm spectral channel is 322.34 nm. This means the monochromatic spectral radiance calculated at 322.34 nm can represent the radiance of the 322.5 nm spectral channel, which has 0.6 nm (FWHM) resolution with an error value of less than 0.1 %. As the instrument has twice as high spectral resolution as TOMS, one point (effective center wavelength) within one spectral channel is enough to represent the convoluted value instead of 5 points in ADEOS TOMS case.

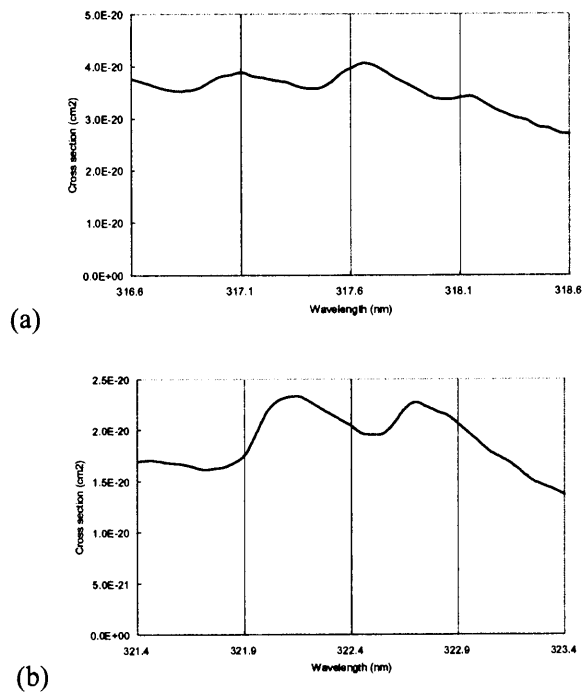

Figure 4-26. O_3 absorption cross-section at 273.15 K by *Bass et al.* [1985] and corrected by K. Chance [private communication, 2002]: (a) around 317.6 nm and (b) 322.4 nm.

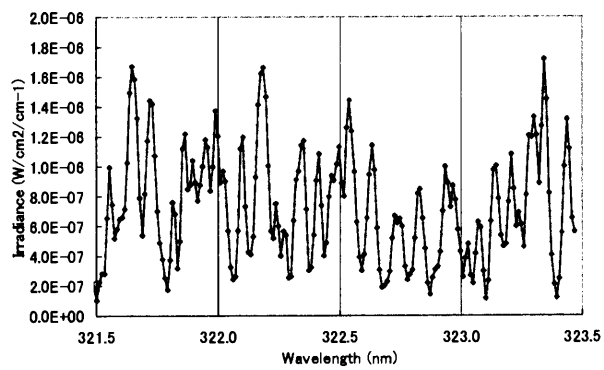

Figure 4-27. Fraunhofer spectra around 322.5 nm [*Berk et al.*, 1989].

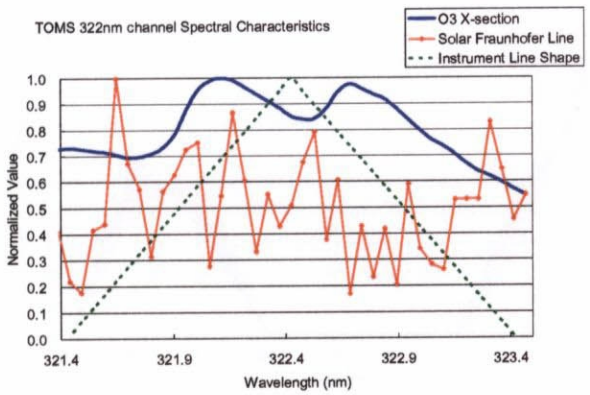

Figure 4-28. Spectral characteristics near 322 nm of O_3 absorption cross section, solar spectral Fraunhofer line and instrument line shape function.

The slit function (instrument function) represents the spectral response of the instrument. In the above method, the slit function must be characterized accurately. Figure 4-29 shows the slit function of the laboratory model measured with a 1m monochromator and a Xe lamp light source. Figure 4-30 shows the simulated sensitivity to the wavelength shift onboard using a Hg lamp calibration source. These results indicate that the polychromator has a uniform slit function over the wide spectral range and its center wavelength can be well calibrated. In addition, the spectrometer is controlled to keep the temperature change less than 1 degree C. The wavelength shift due to the temperature change during the Hg lamp calibration is less than 0.01 nm. Thus the polychromator will provide well wavelength-calibrated data over the entire mission.

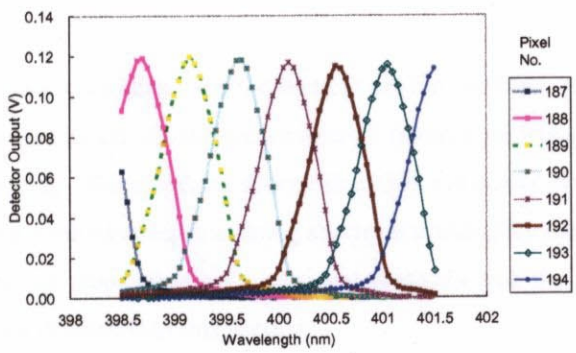

Figure 4-29. The laboratory-model measurement of slit function without depolarizer using the 1m monochromator.

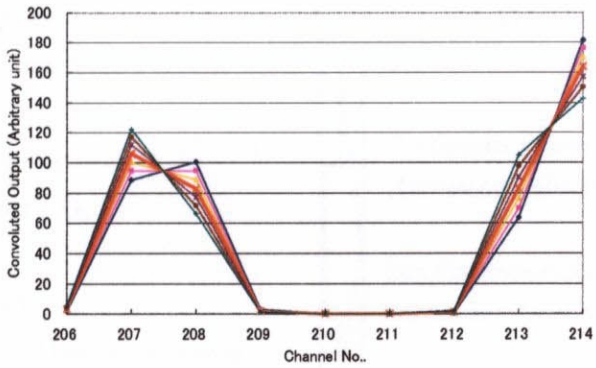

Figure 4-30. Hg lamp (404.66 nm and 407.78 nm) sensitivity on the wavelength shift (nominal, +/-1,2,3 cm^{-1}).

Pair selection and optical thickness. The total O_3 can be retrieved using one of the several pairs of O_3 sensitive and insensitive spectral channels. As discussed in 4.5.1, the spectral channels suitable for the O_3 retrieval must have an optical thickness between 0.5 and 2, which has moderate absorption. The optical thickness is defined as the product of the air mass factor (the solar zenith angle and the viewing angle), the O_3 amount on the path, and the O_3 absorption cross section. When the optical thickness is too large, the measured spectra are weak and the SNR becomes low. On the other hand, the channel that has small optical thickness is O_3 insensitive. Several pairs that have medium moderate optical thickness will be selected depending on the observation geometry in the data processing. Each pair will be weighed based on the error value.

4.5.2. Tropospheric O_3 Retrieval

(1) Previous method

Shorter wavelength regions have been used for vertical profile retrieval, such as with SBUV and GOME. High spatial resolution is required to satisfy the recent interest monitoring tropospheric O_3, which is related to air pollution and biomass burning. Solar spectra shorter than 300 nm rarely penetrate into the troposphere or surface, and therefore the some method other than using shorter wavelength must be investigated. Figure 4-31 schematically illustrates previous tropospheric O_3 retrieval methods and the expected improvement. The details of the new algorithm are discussed in this section.

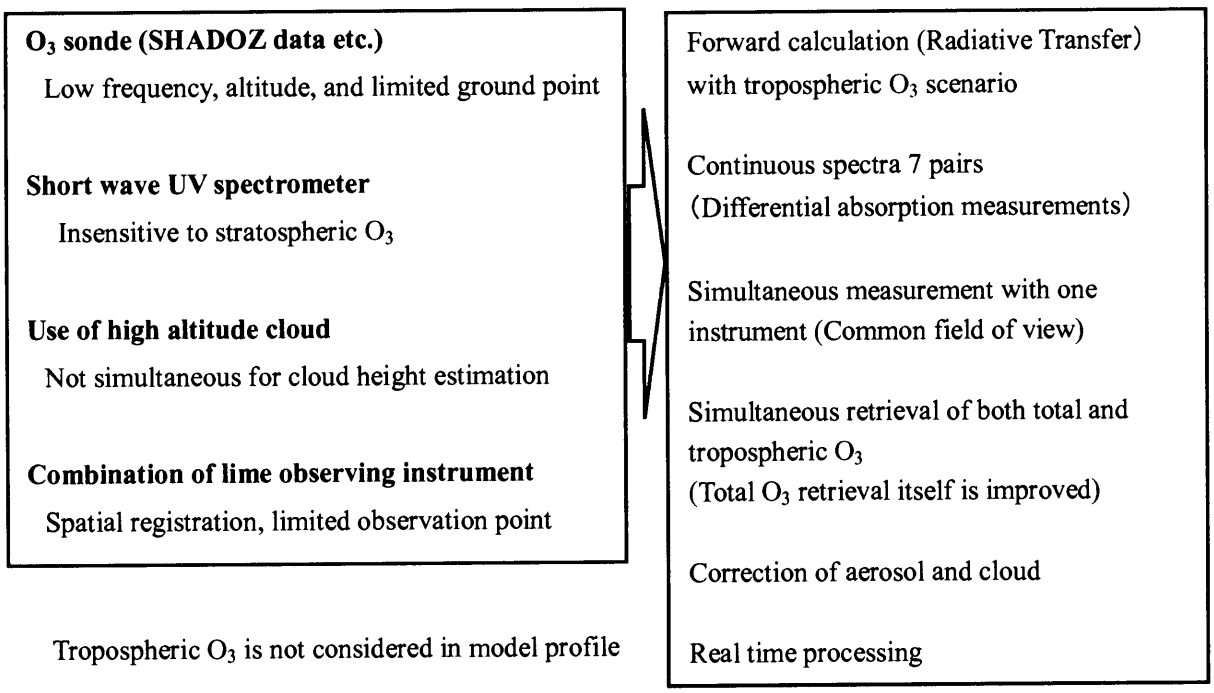

Figure 4-31. Past tropospheric O_3 retrieval and its improvement.

(2) SBUV retrieval

SBUV instruments on NIMBUS 7 and NOAA satellites used shortwave UV backscattered spectra for stratospheric O_3 vertical profile retrieval. Figure 4-32 depicts the simulated contribution function of the shortwave UV. The contribution function can be defined as follows.

$$C = \frac{\partial y}{\partial \log p} = p \exp\left[-s_2\left(\int_0^p \alpha_{px} x_{p_o} dp_O + \beta_\lambda p\right)\right], \tag{4-13}$$

The vertical profile of stratospheric O_3 can be retrieved with a height resolution of about 5 km height if the backscattered UV spectra are shorter than 300 nm as indicated Figure 4-32. However, there is no contribution from tropospheric O_3. The total O_3 is first retrieved using a longer wave channel for vertical profile retrieval and the estimated total O_3 is used as constraint for the profile inversion. Accurate total O_3 retrieval requires the tropospheric O_3 information since the longer wave UV spectra are sensitive to lower atmosphere. Therefore, another retrieval method must be investigated.

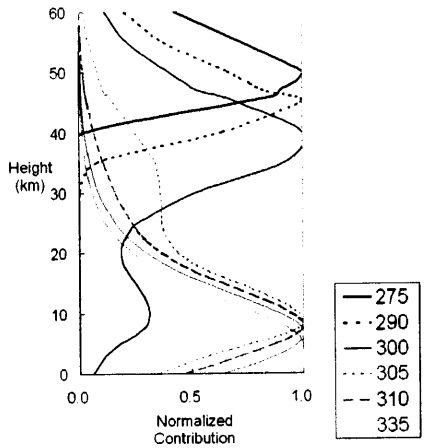

Figure 4-32. Contribution function of the shortwave UV (275, 290, 300, 305, 310, and 335 nm).

(3) O_3 vertical profile

In Chapter 2, for the TOMS observation, in the condition of the O_3 vertical profile, error between pairs is minimized. The spectral dependency of the solar flux penetration and the temperature dependency of the O_3 absorption cross section can be used for the separation of stratospheric and tropospheric O_3. The solar flux of the longer wavelength penetrates into the lower atmosphere because the Rayleigh scattering coefficient and O_3 absorption cross section become small. Figure 4-33 shows the acquired optical thickness in the observation geometry. Figure 4-34 shows an O_3 absorption cross section model of three altitudes. It has a peak and bottom structure. The absorption cross section peak has less temperature dependency than the bottom. This means that using the pair method, the O_3 differential absorption is weaker near the surface than in the stratosphere. As several pairs can be selected in the spectral range, the instrument is expected to provide more information on the O_3 distribution than TOMS.

Now let us examine the feasibility of the tropospheric O_3 retrieval with a model sensitivity study. Figure 4-35 shows the example of tropospheric O_3 vertical profile based on sonde data acquired at Watukosek, Indonesia and Nairobi [*Thompson et al.*, 2003]. The data shows maxima in troposphere of O_3 vertical profile. The vertical profile models including the polluted model of the troposphere will be added as shown in Figure 4-36.

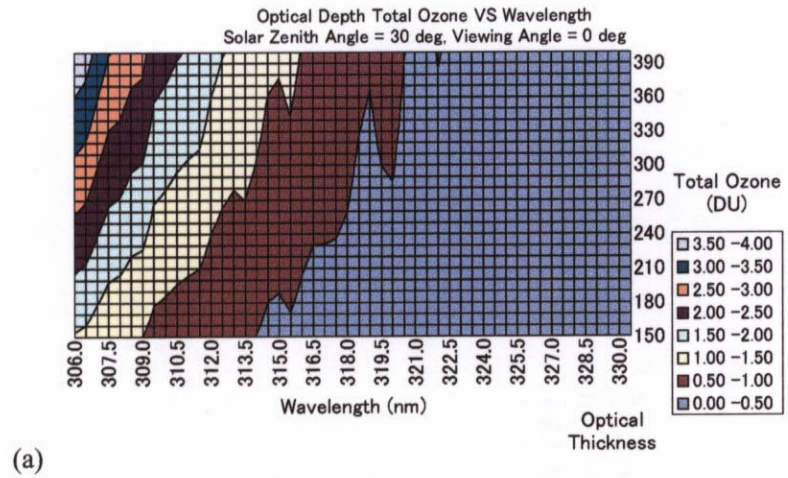

(a)

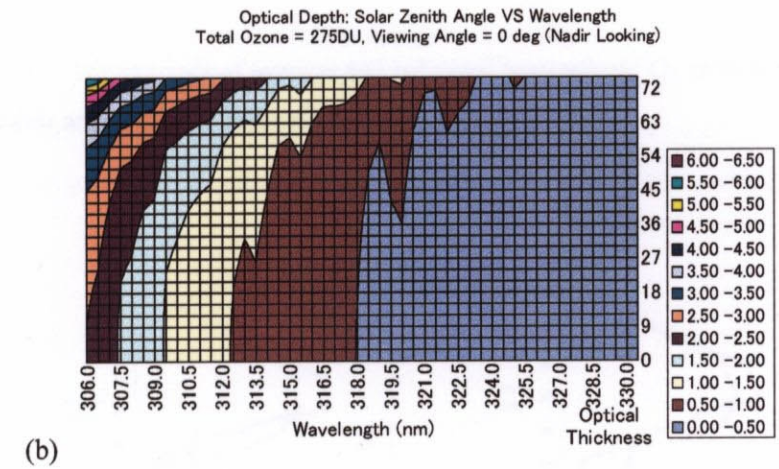

(b)

Figure 4-33. Optical thickness acquired in observation geometry as function of (a) wavelength and the total O_3 (b) wavelength and solar zenith angle.

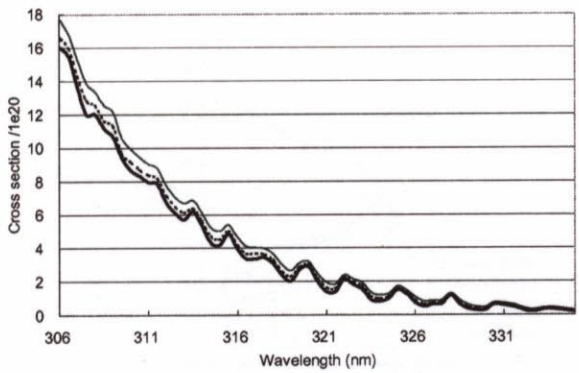

Figure 4-34. O_3 absorption cross-section model of the surface (solid line), 5 km (dotted line), and 30 km (bold line).

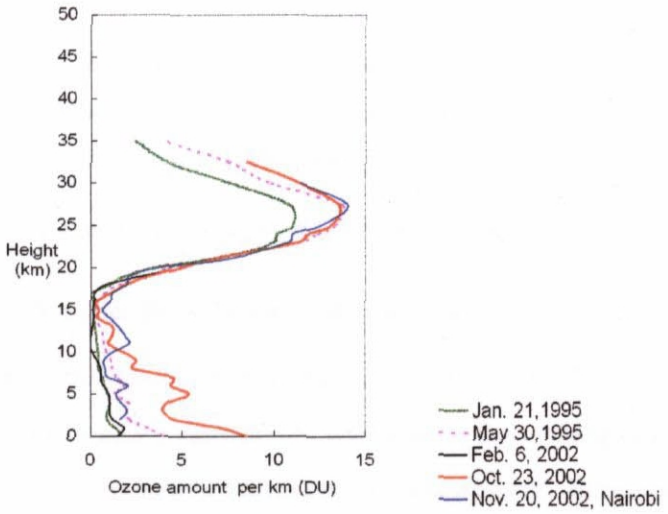

Figure 4-35. The example of average and enhanced tropospheric O_3 vertical profile based on sonde data acquired at Watukosek, Indonesia, and Nairobi.

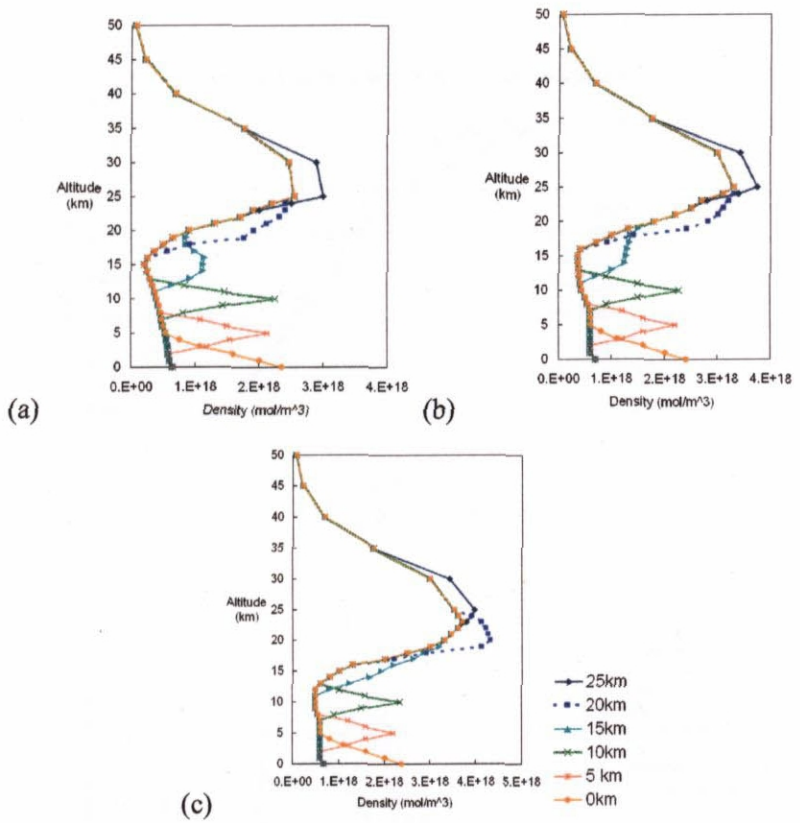

Figure 4-36. O_3 vertical profile models in case of the total O_3 275 DU. The solid line represents the typical low latitude model, and the bold, dash-dotted and dotted lines represent the polluted O_3 models of the troposphere: (a) total O_3 of 225 DU, (b) 275 DU and (c) 325 DU.

(4) Forward calculation

The scattered radiance in this model is calculated using the following equation assuming single scattering. The temperature dependency data of the O_3 absorption cross section acquired by *Molina et al.* [1986] and the Rayleigh scattering ratio model by *Bucholtz* [1995] are used.

$$\frac{4\pi I_\lambda}{F_\lambda} = \beta_\lambda P(cos\theta)\int_0^1 s_1\, exp\left[-s_2\left(\int_0^p \alpha_{px} x_{p_o}\, dp_O + \beta_\lambda p\right)\right]dp + R_\lambda\, exp\left(-\left(\int_0^p \alpha_{px} x_{p_o}\, dp_O + \beta_\lambda\right)\right), \qquad (4\text{-}14)$$

where θ_i is the solar zenith angle, β_λ is the Rayleigh scattering coefficient, $P(\cos\theta_0)$ is the Rayleigh phase function, x is the O_3 density, p is the pressure, and R_λ is surface albedo. The optical path (air mass) factors s_1 and s_2 are $\sec(\theta_v)$, and $\sec(\theta_v)+\sec(\theta_s)$ respectively, where θ_v is the viewing angle. Figure 4-37 shows the model-calculated sensitivity of the earth's albedo on O_3 vertical model difference. In addition, the earth's albedo is divided by the adjoining the O_3 insensitive channels as shown in Figure 4-38. These results show that the shorter wavelength channels are more sensitive to the troposphere/stratosphere O_3 discrimination because the penetration altitudes differ in wavelength. They also indicate that in longer wavelength channels, the tropospheric O_3 has larger sensitivity due to the temperature dependency of the O_3 absorption cross section.

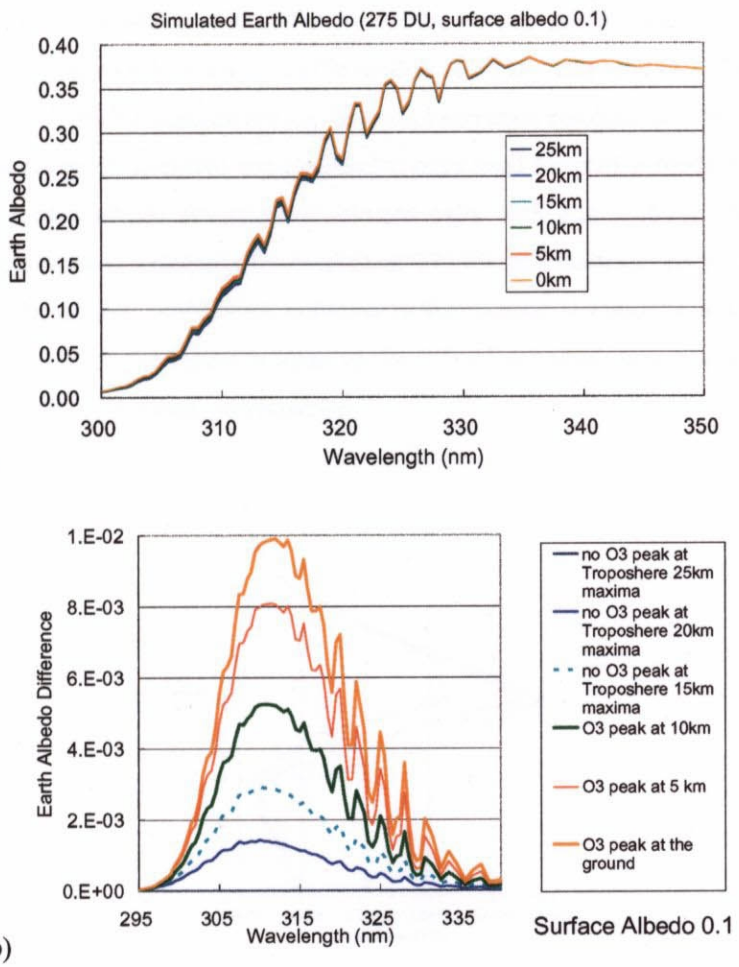

Figure 4-37. (a) The model calculated earth's albedo on O_3 vertical model difference and (b) their deviation from the 25 km peak model.

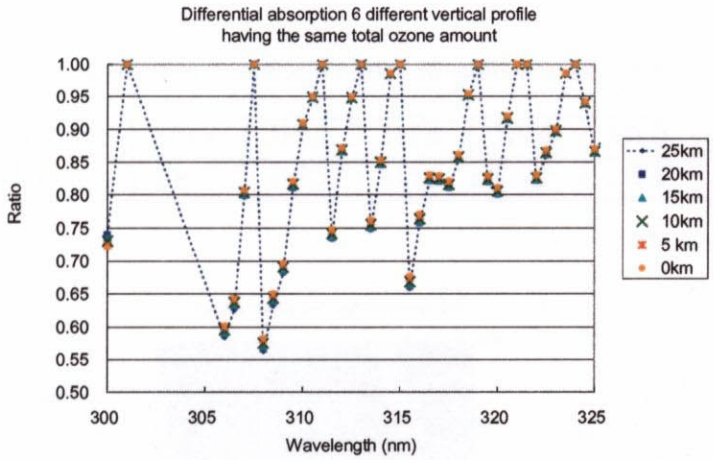

Figure 4-38. The same as Figure 4-37 except that the calculated earth's albedo is divided by the adjoining O_3 insensitive channels (301.0, 307.5, 311.0, 313.0, 315.0, 319.0, 321.5, 324.0, 326.5, 329.5, 332.5, and 335.5 nm).

(5) Retrieval

The look-up tables for the total O_3 (50 DU step) and the vertical profile models of tropospheric O_3 have been prepared. Figure 4-39 shows the vertical profile models of 50 DU step total O_3. The total O_3 and vertical profile model combination, which minimize the model and observation residual, will be selected using spectral pairs. Table 4-8 shows seven O_3 sensitive and insensitive pairs used for profile model retrieval. Figure 4-40 shows the sum of the earth's albedo deviation of selected pairs with and without 300 and 301 nm. It is minimized in the fitting process to determine the total O_3 of 275 DU and the tropospheric O_3 vertical model that has the peak at 5 km. The proper combination is deeper in the contour plot and the solution is unique in both cases. The deviation of 0.25 in the figure is equal to the 1 % observation error, the level of which is about twice as large as the expected instrument performance.

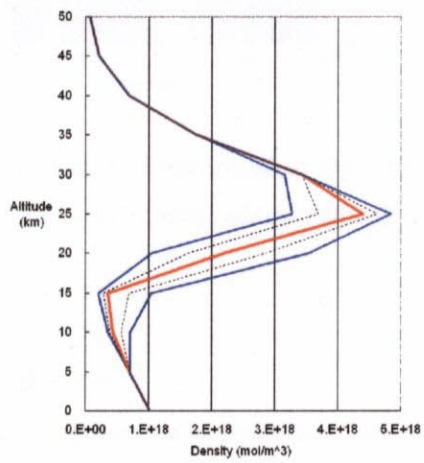

Figure 4-39. O_3 vertical profile models for the total O_3 of 225, 250, 275, 300, and 325 DU (from left to right).

Table 4-8. Seven O_3 sensitive and insensitive pairs for profile model retrieval.

O_3 insensitive channel (nm)	310.0	313.0	315.0	319.0	321.0	324.0	326.5
O_3 sensitive channel (nm)	306.0	313.5	315.5	320.0	322.0	325.0	328.0

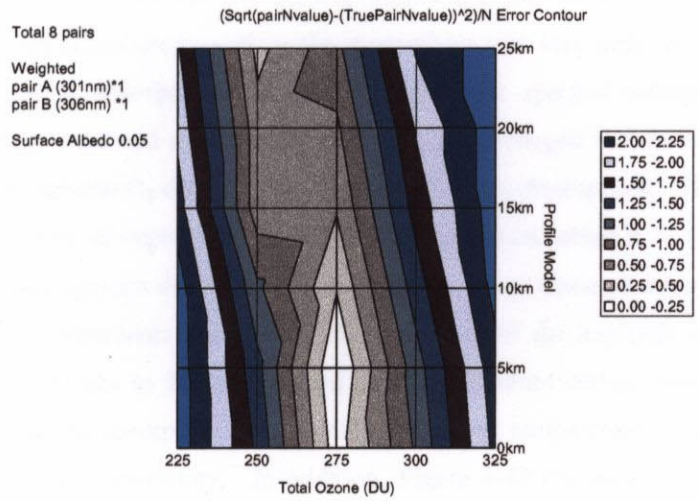

(a)

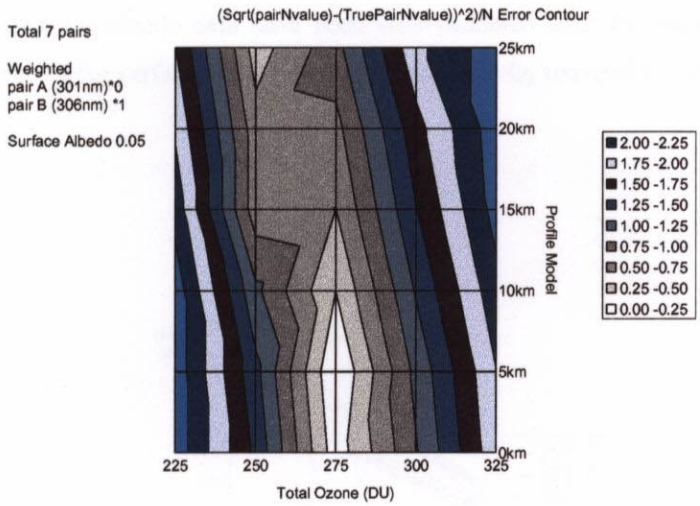

(b)

Figure 4-40. The deviation, which is minimized in the fitting process to determine the total O_3 and profile model: (a) with 8 pairs (adding 300 nm and 301 nm pair) and (b) 7 pairs.

(6) Origins of backscattered radiation

Figure 4-41 and Figure 4-42 designate the contribution and weighting functions of the different wavelengths. The weighting function can be defined as follows.

$$W = \frac{\partial z}{\partial x_p}, \tag{4-15}$$

where $z = \frac{4\pi I_\lambda}{F_\lambda} = \beta_\lambda P(cos\theta)\int_0^1 s_1 \, exp\left[-s_2\left(\int_0^p \alpha_{px} x_{p_o} dp_O + \beta_\lambda p\right)\right]dp + R_\lambda \, exp\left(-\left(\int_0^p \alpha_{px} x_{p_o} dp_O + \beta_\lambda\right)\right)$.

When we expand the spectral coverage to shorter wavelengths, the scattering contribution of the shorter wavelength spectra is mainly from the stratosphere. Therefore shorter wavelength spectra are suitable for stratospheric O_3 estimation and it will be possible to extract the stratospheric O_3 from the total value. However, backscattered light at 300 nm penetrates into the troposphere and still contains information of tropospheric O_3. Penetrated light at 295 nm is scattered mostly in the stratosphere with very little contribution to tropospheric O_3. Shorter wavelength light is absorbed strongly by O_3, and solar spectral radiance itself is weak; thus the scattered radiance is very weak and signals must be added and averaged to improve the SNR. However, the spatial scale of the stratospheric O_3 distribution is larger than in the troposphere. Therefore, adding the shorter wavelength region would be an improvement if the satellite resources permit it.

The weight of each spectra decreases gradually in the lower atmosphere, as indicated in Figure 4-42. The spectral dependency represents the spectral characteristics of the Rayleigh scattering coefficient. The weighting function of 330 nm in Figure 4-42 (a) exhibits different curves from other wavelengths. The differences exist because the absorption cross section has strong temperature dependency at 330 nm and O_3 near the tropopause has less sensitivity. In addition, Figure 4-42 (b) specifies the weighting functions of different surface albedo. The difference is very small. In general, the surface albedo in the UV region is small, and the global surface albedo data have been well validated after 20 years of TOMS measurements. The effect of uncertainty of the surface albedo on the tropospheric O_3 retrieval is considered to be small.

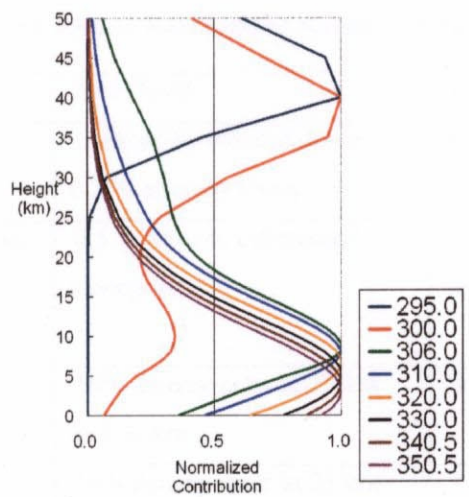

Figure 4-41. Normalized contribution function of the different wavelength in case of total O_3 amount 275 DU, solar zenith angle = 30 deg and viewing angle = 30 deg.

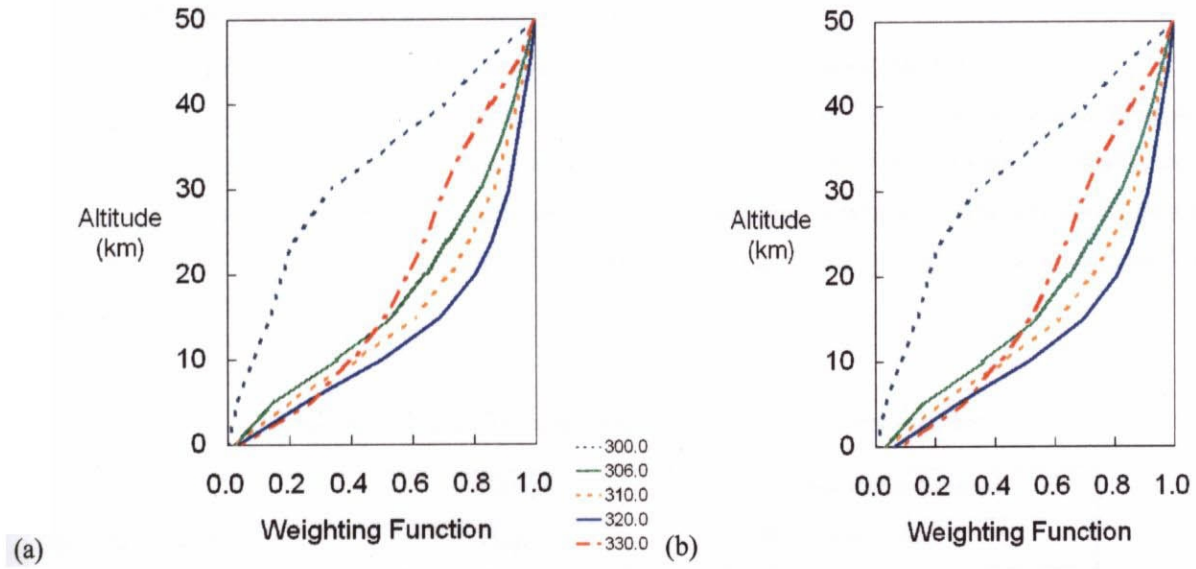

Figure 4-42. Normalized weighing function of the earth albedo for total O_3 amount 275 DU, solar zenith angle = 30 deg and viewing angle = 30 deg: (a) surface albedo of 0 and (b) 0.1.

(7) Error estimation

The major error sources and expected accuracy are summarized in Table 4-9. The error due to inaccuracies in surface albedo, *a priori* information, and the stratospheric O_3 profile are also estimated.

Table 4-9. The major error sources and expected accuracy of tropospheric O_3 retrieval.

Error source	Error level	Error effect
Aerosol	1% (can be reduced down to 0.2 % error by correction)	Smaller than noise level
Temperature dependency of cross section 0.26% error per K at 315.5 nm	0.5 % error in differential absorption	5 km vertical profile (1 Umkehr layer) error in troposphere
Stratospheric O_3 profile	10% density error in 25 km and 30 km	Smaller than noise level
	50% density error in 25 km and 30 km	2.5 km vertical profile (0.5 Umkehr layer) error in troposphere
Surface albedo	*A priori* 0.05 (true 0)	Smaller than noise level
	A priori 0.05 (true 0.3)	2.5 km vertical profile error in troposphere